ACCOUNTS
of chemical research

Advances in Solid-State Relaxation Methodology for Probing Site-Specific Protein Dynamics

JÓZEF ROMUALD LEWANDOWSKI
Department of Chemistry, University of Warwick, Coventry CV4 7AL, U.K.

RECEIVED ON DECEMBER 16, 2012

CONSPECTUS

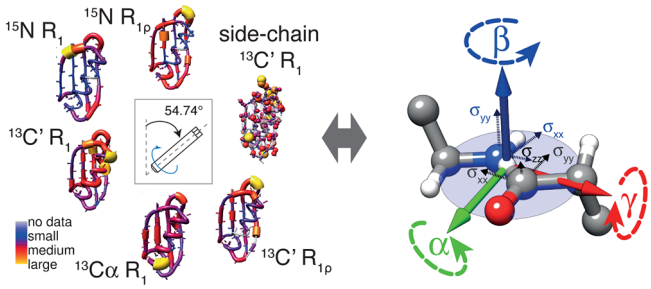

Dynamics are intimately linked to protein stability and play a crucial role in important biological processes, such as ligand binding, allosteric regulation, protein folding, signaling, and enzymatic catalysis. Solid-state NMR relaxation measurements allow researchers to determine the amplitudes, time scales, and under favorable conditions, directionality of motions at atomic resolution over the entire range of dynamic processes from picoseconds to milliseconds. Because this method allows researchers to examine both the amplitudes and time scales of motions in this range, they can link different tiers of protein motions in protein energy landscapes. As a result, scientists can better understand the relationships between protein motions and functions. Such studies are possible both with the primary targets of solid-state NMR studies, such as amyloid fibrils, membrane proteins, or other heterogeneous systems, and others that researchers typically study by solution NMR and X-ray crystallography. In addition, solid-state NMR, with the absence of tumbling in solution, eliminates the intrinsic size limitation imposed by slow tumbling of large proteins. Thus, this technique allows researchers to characterize interdomain and intermolecular interactions in large complexes at the atomic scale.

In this Account, we discuss recent advances in solid-state relaxation methodology for studying widespread site-specific protein dynamics. We focus on applications involving magic angle spinning, one of the primary methods used in high-resolution solid-state NMR. We give an overview of challenges and solutions for measuring ^{15}N and ^{13}C spin−lattice relaxation (R_1) to characterize fast picosecond−nanosecond motions, spin−lattice in the rotating frame ($R_{1\rho}$), and other related relaxation rates for characterization of picosecond−millisecond protein motions. In particular, we discuss the problem of separating incoherent effects caused by random motions from coherent effects arising from incomplete averaging of orientation-dependent NMR interactions. We mention a number of quantitative studies of protein dynamics based on solid-state relaxation measurements. Finally, we discuss the potential use of relaxation measurements for extracting the directionality of motions. Using the ^{15}N and ^{13}C R_1 and $R_{1\rho}$ measurements, we illustrate the backbone and side-chain dynamics in the protein GB1 and comment on this emerging dynamic picture within the context of data from solution NMR measurements and simulations.

Introduction

The view of proteins as functional nanomachines is an attractive notion for many biologists. In this view, the three-dimensional structure of a protein encodes its intrinsic mechanical properties that determine how the structure evolves in time to accomplish a specific task. Dynamics play a crucial role in many important biological processes, such as ligand binding, allosteric regulation, protein folding, signaling, and enzymatic catalysis.[1] Flexibility is also intimately linked to protein stability. A complex multidimensional energy landscape is required to describe and understand the protein states sampled by thermal fluctuations.[2]

Published on the Web 04/26/2013 www.pubs.acs.org/accounts
10.1021/ar300334g © 2013 American Chemical Society

Experimental characterization of such a landscape is a challenging task and requires a diverse set of tools. The time scales of dynamics often dictate the methodology used to characterize them (see Figure 1). NMR is an important approach to accomplish this task because it provides information on motions at the atomic resolution. Relaxation measurements, the focus of this Account, allow characterization of time scales, amplitudes, and sometimes directionality of the motions. The precise range of applicability for relaxation is different in solution and solid state. In solution, relaxation methods report on motions from picoseconds to the correlation time of the overall rotational diffusion (correlation time increases with the size of protein but generally falls within the picosecond−nanosecond range). Nanosecond to millisecond motions may be probed in solution only by alternative methods; for example, amplitudes of motions may be measured with residual dipolar couplings (RDC) in anisotropic liquids, and microsecond to millisecond motions may be probed by exchange methods.[3] However, none of these methods yield simultaneously time scales and amplitudes of motions. In the solid state where overall tumbling is absent, the relaxation may be used to characterize *amplitudes and time scales of motions from picoseconds to milliseconds* and thus gives access to important biological dynamic processes in the range from bond fluctuations to folding events (see Figure 1), notably including the nanosecond−microsecond "blind" spot for the solution NMR relaxation. Furthermore, the absence of overall tumbling in the solid state removes the intrinsic limitation on the size of proteins that can be studied by NMR. Large proteins tumble slowly in solution, which leads to efficient transverse relaxation coupled with broadening of the lines and a decrease in sensitivity. In the solid state, this source of relaxation is generally absent. Consequently, provided that the problems of sensitivity as well as solid-state specific line broadening and spectral crowding are addressed, solid-state NMR (SSNMR) could be used to study structure and site-specific dynamics even for very large systems. As the current focus of biology shifts from looking at isolated parts of systems to considering interactions of these parts in the context of more complete assemblies, such SSNMR applications are becoming increasingly important.

In this Account, we discuss recent advances in SSNMR relaxation methodology for studying widespread site-specific protein dynamics. We focus on applications involving magic angle spinning (MAS), which is one of the primary approaches for high-resolution SSNMR. We highlight the benefits of ^{15}N and ^{13}C relaxation measurements and how they complement information available from other techniques. We also consider some of the remaining challenges for the field and possible future directions.

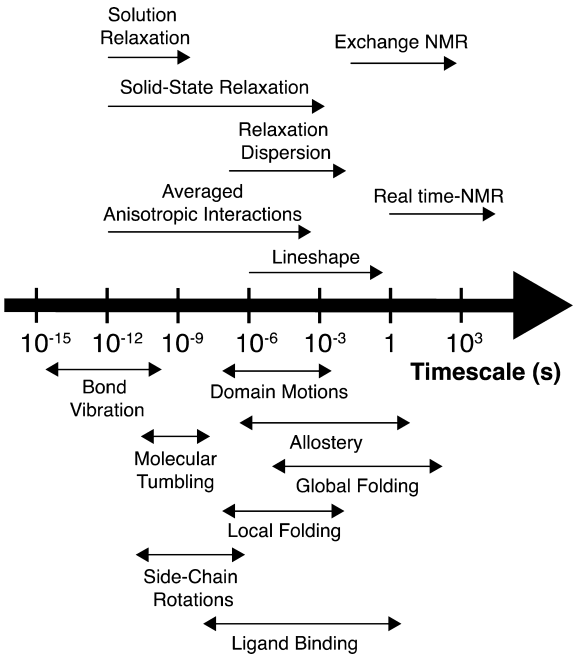

FIGURE 1. Examples of dynamic processes in proteins and NMR approaches to probe them.

Sample Preparation

Isotopic labeling is usually required for NMR relaxation measurements and is typically achieved by overexpression of recombinant proteins in isotopically (e.g., ^{15}N, ^{13}C, ^{2}H) labeled media.[4] Customizing the labeling patterns is helpful in manipulating the spin dynamics, for example, turning "on" and "off" NMR interactions whose fluctuations contribute to relaxation (e.g., dipolar couplings). Another prerequisite for site-specific relaxation measurements is appropriate preparation of a hydrated solid-state sample that yields spectra with resolved individual sites. Here, progress has been made thanks to the popularization of nanocrystalline protein preparations.[5] However, a particular strength of SSNMR is that long-range order granted by crystallinity is not a requirement for obtaining high-quality NMR spectra. The only requirement is local order, which is often easier to achieve. This feature grants access to atomic resolution structural and dynamic information for systems such as fibrils or supramolecular assemblies, for example, type III secretion needle.[6,7] Recently, sedimentation by ultracentrifugation was introduced as a simple way of preparing samples yielding spectra rivaling the quality of spectra from good crystalline preparations.[8] Sedimentation works well on large protein systems, which creates new exciting opportunities for SSNMR studies of protein complexes.

Protein Dynamics and Magic Angle Spinning

Characterization of the complex hierarchy of motions requires a number of independent measurements. Currently, the solid-state relaxation methodology toolbox is still not as rich as its solution-state equivalent. For example, to date there is no practical method for measuring site-specific ^{15}N NOE in the solid state even though it is routinely used for characterizing fast motions in solution (though ^{15}N heteronuclear NOE has been observed in the solid state[9]). One of the main reasons behind the scarcity of appropriate methods is that relaxation rates measured in the solid state are generally affected not only by incoherent processes such as random thermal fluctuations (which is the case in solution) but also coherent processes originating from the incomplete averaging of strongly coupled networks of anisotropic interactions in solid proteins. Anisotropic NMR interactions, such as dipolar coupling (direct through space interaction of two magnetic nuclear dipoles), chemical shift (local, induced magnetic field experienced by a nucleus due to orbiting electrons), and quadrupolar coupling (electric interactions of spin $I > 1/2$ nuclei with the surrounding electric fields), depend on their orientation with respect to the external magnetic field. In solution, overall rotational diffusion of the molecules causes all the possible orientations to be sampled in a very short period of time (average time for rotation by 1 rad, that is, correlation time, is on the order of picoseconds to nanoseconds). This leads to the complete averaging of the anisotropic interactions and narrow resonances in NMR spectra (only the isotropic, that is, independent of orientation, parts of chemical shift and *J* coupling are observed). In solids, the absence of overall tumbling means an absence of such motional averaging (though occasionally extensive local motions also completely average anisotropic interactions in solids, for example, see ref 10). In static solids, molecules usually are immobilized in many different orientations with respect to the external magnetic field. Each orientation yields a spectrum at a specific frequency; therefore, summation over all the possible orientations results in broad lines on the order of kilohertz to megahertz. One of the approaches to remove such anisotropic broadening involves mechanical rotation of the samples under the so-called magic angle (magic angle of ~54.736°, a value for which the second-order Legendre polynomial describing the orientational dependence of dipolar coupling and chemical shift anisotropy (CSA) becomes zero) with respect to the external magnetic field. The efficiency of the suppression of anisotropic interactions depends on their nature and the ratio of their magnitude to the spinning frequency (to attain efficient suppression the spinning frequency, ν_r, has to be higher than the magnitude of the interaction, motivating development of fast MAS technology). In proteins, homonuclear ^{1}H−^{1}H dipolar couplings are some of the most difficult interactions to suppress by spinning due to their large magnitude and homogeneous nature (for three or more protons the dipolar Hamiltonian does not commute at different time points, which makes it very difficult to average out). For example, even with the currently highest available ν_r of 110 kHz (the maximum achievable ν_r depends on the diameter of the rotor/sample holder, which has to be as small as 0.75 mm to reach 110 kHz), ^{1}H−^{1}H couplings are still not as well suppressed by MAS as they are by the tumbling in solution (but sufficiently to enable sensitive ^{1}H-detected experiments, for example, see ref 11). Even though NMR relaxation is induced by incoherent random motions modulating anisotropic interactions (random motions are incoherent because the precise moment at which each molecule in an ensemble changes its state is unpredictable), the incompletely averaged interactions may have a similar effect on the experiments (even though this effect does not originate from molecular motions). For example, a coherent dipolar dephasing process is difficult to distinguish from the decay of transverse magnetization due to incoherent relaxation (dipolar dephasing is a coherent process because it is the same for all the molecules of certain type in the ensemble). Experimental ambiguity between incoherent and coherent effects poses a serious challenge for relaxation measurements in the solid state. Fortunately, this challenge can often be addressed through sample preparation or careful experimental design. In the following sections, we discuss approaches for dealing with coherent processes during measurements of solid-state relaxation rates.

Accessing Picosecond−Nanosecond Motions: Overcoming Averaging of Spin−Lattice Relaxation Rates due to Spin Diffusion

One of the main challenges for measuring site-specific solid-state spin−lattice relaxation rates (denoted R_1) reporting on picosecond−nanosecond motions is a *coherent* process called spin diffusion. Spin diffusion originates from dipolar couplings and promotes spontaneous exchange of magnetization between spins (note that in solution NMR the term spin diffusion is used to describe polarization transfer relayed through intermediate spins due to the *incoherent* cross-relaxation process). If during an R_1 measurement (which involves following the magnitude of *z*-magnetization, that is,

aligned with the magnetic field, as function of relaxation delay) magnetization between different sites is exchanged sufficiently fast compared with the relaxation times due to spin diffusion, then the measured relaxation rates are averaged over several sites. In extreme cases such as measurements of ^{13}C R_1 in uniformly ^{13}C labeled proteins at $\nu_r < 20$ kHz, the recorded rates are averaged over several backbone and side chain sites rendering them unusable for quantitative characterization of site-specific protein dynamics. Fortunately, spin diffusion rates are reduced by increasing ν_r, radiofrequency (rf) averaging, or dilution of the $^1H-^1H$ spin network through replacing protons with deuterium atoms. Dilution of ^1H spins and averaging by MAS are the more common of the three approaches. Averaging by rf is less common because it often requires high nutation frequencies that can be detrimental to equipment (due to its limited power handling) and samples (due to rf-induced heating that may, for example, denature a protein). At the same time, application of insufficiently high nutation frequencies may actually assist the spin diffusion. For example, this principle is the basis for a popular method for $^{13}C-^{13}C$ magnetization transfer called DARR.[12]

In the case of ^{13}C and ^{15}N R_1 measurements, the most efficient variant of spin diffusion is assisted by the dipolar couplings to protons and therefore termed proton-driven spin diffusion (PDSD). The PDSD rates depend on the strength of the involved heteronuclear $^1H-^{13}C/^1H-^{15}N$ and homonuclear $^{13}C-^{13}C/^{15}N-^{15}N$ dipolar couplings and are inversely proportional to the ν_r.[13] In uniformly ^{13}C- and ^{15}N-labeled proteins and at the same ν_r, the rates for $^{15}N-^{15}N$ PDSD are significantly smaller than the rates for $^{13}C-^{13}C$ PDSD because the average $^1H-^{15}N$ and $^{15}N-^{15}N$ dipolar couplings are smaller than the average $^1H-^{13}C$ and $^{13}C-^{13}C$ dipolar couplings. Consequently, site-specific ^{15}N R_1 in fully protonated proteins is readily available from experiments performed at $\nu_r > 20$ kHz but somewhat affected by PDSD for experiments performed in the $\nu_r = 10-20$ kHz range.[14−16] Slow $^{15}N-^{15}N$ PDSD is one of the main reasons why ^{15}N R_1 measurements were some of the first relaxation measurements adopted for quantitative description of widespread site-specific dynamics in the solid state.[17]

Recently, Lewandowski et al. showed that $\nu_r \geq 60$ kHz is required to enable site-specific ^{13}C R_1 measurements in uniformly ^{13}C-labeled proteins.[18] At $\nu_r = 60$ kHz, the PDSD is much better suppressed for $^{13}C'$ than side-chain ^{13}C R_1 measurements, which may need to be taken into account for quantitative analysis.[18] In addition, PDSD rates are significantly reduced in samples where the proton−proton network is diluted by substituting deuterium for protons.[16,19]

Characterizing Slow Nanosecond−Millisecond Motions: Can We Measure Spin−Spin Relaxation in the Solid State?

^{15}N and ^{13}C R_1 measurements are sensitive reporters on molecular motions occurring on a few dozens of picoseconds to a few dozens of nanoseconds (except for the $^{13}C-^{13}C$ dipolar contribution to ^{13}C R_1, which is weakly sensitive to slower motions[20]). However, in order to take full advantage of the expanded range of applicability of relaxation methods in the solid state, measurements of parameters sensitive to slow (i.e., nanosecond−millisecond in this context) motions, such as the spin−spin relaxation (R_2) or the spin−lattice relaxation in the rotating frame ($R_{1\rho}$), are indispensable. One of the main challenges for measuring R_2 to characterize motions in solids is that coherent effects, particularly dipolar dephasing, typically dominate the decay of transverse (i.e., perpendicular to the magnetic field) magnetization. Since the largest coherent contribution to the decay of transverse magnetization originates from strong dipolar $^1H-^1H$ couplings, the situation improves in perdeuterated proteins in which hydrogen atoms are replaced with deuterium atoms (the gyromagnetic ratio of ^2H is ~6.5 times smaller than that of ^1H resulting in $\sim 6.5^2$ times weaker dipolar couplings and reduced dephasing). A popular approach to achieve this relies on growing bacteria in D_2O and then reintroducing protons only at exchangeable sites (primarily amide protons) by means of recrystallizing/precipitating the protein from a buffer containing a varying ratio of H_2O and D_2O (e.g., using 10% H_2O and 90% D_2O to obtain 10% reintroduction of exchangeable protons).[21]

Even though perdeuteration significantly reduces the coherent contribution to transverse relaxation rates, under most currently available experimental conditions such a contribution still remains non-negligible compared with the incoherent motion-induced contribution. For example, the coherent contribution to the average R_2' rate measured in a spin−echo experiment at $\nu_r = 60$ kHz in a perdeuterated protein with 10% exchangeable protons may easily be greater than 75% of the measured rate.[22] Consequently, so far R_2' is used to only *qualitatively* characterize protein dynamics. However, the long coherence lifetimes afforded by perdeuteration facilitate related approaches that provide a *quantitative* measure of dynamics.

One such approach suggested by Chevelkov et al. relies on a measurement of ^{15}N dipolar-CSA cross-correlated

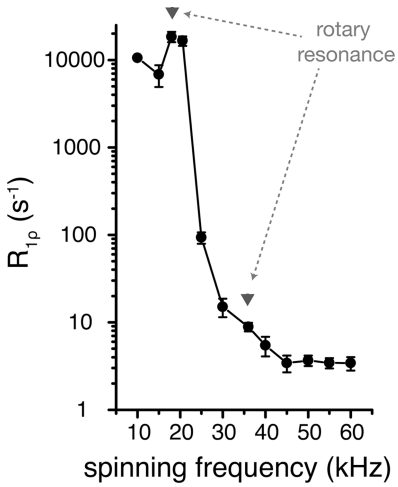

FIGURE 2. Overall amide ^{15}N $R_{1\rho}$ in [U-^{13}C,^{15}N]-GB1 as a function of spinning frequency at an ^{15}N spin-lock amplitude of 18 kHz and ^{1}H Larmor frequency of 500 MHz.[22]

relaxation.[23] In this approach, the dynamic information is extracted from a difference between the R_2' rates measured for the two components of the J_{NH} doublet.[23] The coherent contribution to the decay rates for both components of the doublet is, to a good approximation, the same. The difference between measured rates is primarily due to incoherent cross-correlated relaxation and thus reports on dynamics even though the rates themselves are still dominated by the coherent contribution. A similar approach based on difference in multiple-quantum coherence decays was also introduced recently.[24]

In the presence of chemical exchange, the coherent contribution to R_2 in perdeuterated proteins is usually smaller than the exchange contribution to R_2. Recently, Tollinger et al. used this feature to quantify microsecond to millisecond motions in ubiquitin by means of Carr−Purcell−Meiboom−Gill (CPMG) relaxation dispersion.[24] In this experiment, $R_{2,\mathrm{eff}}$ is measured as a function of CPMG frequency that is determined by the spacing between series of 180° pulses. The obtained relaxation dispersion profiles contain effects of both chemical exchange and averaging of the coherent residual. However, the dispersion due to the coherent residual is minimal compared with the dispersion due to chemical exchange. Consequently, fitting the dispersion curves yields information on the chemical exchange process with negligible error from ignoring the coherent contribution.

While perdeuteration is a very useful and powerful tool, it is not always necessary for gaining access to relaxation parameters that quantify site-specific slow dynamics. In fact, it is possible to measure $R_{1\rho}$ relaxation rates that are sensitive to picosecond−millisecond motions ($R_{1\rho}$ involves following the magnitude of magnetization locked along a continuous pulse as a function of its pulse duration) under conditions where the coherent contribution is negligible even in fully protonated proteins. A combination of rf and MAS averaging afforded by a >10 kHz ^{15}N spin-lock pulse and $\nu_r > 45$ kHz provides an effective way of reducing the coherent contribution to the $R_{1\rho}$ to a negligible level (in Figure 2, the plateau for the overall ^{15}N $R_{1\rho}$ as a function of ν_r in GB1 indicates settings where efficient averaging of the coherent contribution renders it negligible; rotary resonance conditions where the spin-lock nutation frequency matches ν_r and $2\nu_r$ also have to be avoided). Consequently, measurements of ^{15}N $R_{1\rho}$ provide a direct measure of slow nanosecond−millisecond motions even in fully protonated proteins (this becomes particularly important when high cost and reduced expression yields for perdeuterated preparations render them impractical). As a side note, fast spinning seems indispensable for eliminating the coherent contribution to $R_{1\rho}$ even in perdeuterated proteins. For example, ^{15}N $R_{1\rho}$ rates measured in 10% H_2O [U-^{2}H,^{13}C,^{15}N]SH3 at the same magnetic field and sample temperature are on average ∼2 times smaller at 60 kHz compared with 24 kHz spinning.[22] In general, $R_{1\rho}$ rates may be ν_r dependent,[25] and the mentioned behavior could be reproduced by invoking extremely low amplitude (corresponding to fluctuations of less than 0.5°) microsecond motions. However, bearing in mind that all ^{1}H, ^{15}N, and ^{13}C R_2' still improve in this system with faster spinning and application of decoupling[11] and in the absence of convincing relaxation dispersion data that would demonstrate the presence of such small amplitude slow motions, it is prudent, at least for now, to assume that in the cited case the differences in the measured $R_{1\rho}$ are due to incomplete averaging of the coherent contribution.

Extracting Amplitudes and Time Scales of Motions: Quantitative Analysis of SSNMR Relaxation

The use of SSNMR, and in particular measurements of motionally averaged anisotropic interactions and line shape analysis, to characterize dynamics of proteins in the solid state has a rich history.[26] Dynamics studies have been carried out on a gamut of different samples: fibrils,[27,28] membrane proteins in lipid bilayers,[29] crystals,[30,31] precipitates, etc. However, relaxation-based widespread site-specific quantitative analysis of protein dynamics is a recent phenomenon enabled by the progress in SSNMR methodology. Site-specific measurements of ^{15}N relaxation rates combined with other measurements such as averaged one-bond $^{1}H-^{15}N$ dipolar couplings have enabled quantitative analyses of

protein dynamics in several globular proteins.[17,19,22,32,33] In general, the data are analyzed using Redfield theory-based[34] approaches originally derived for use in solution NMR and modified for use in solids (since the Redfield theory assumption that the root-mean square fluctuation of a perturbation is much smaller than the correlation time may become easily violated in the solid state, we may need to reconsider some of our theoretical approaches in the future). In short, the measured relaxation rates are related to the time scale and amplitude of motion through model-dependent spectral densities that are a measure of motions at correct frequencies to cause transitions between NMR energy levels. A spectral density is a Fourier transform of a correlation function that characterizes the correlation between random fluctuations at different points in time. The amplitudes (often expressed as order parameter S^2 ranging from 1 for a rigid case to 0 for unrestricted motion) and correlation times for the modeled motions are adjusted until the best match to the measured rates is found. The dependence of solid-state relaxation on the orientation of molecules leading to multiexponential decay may be considered explicitly[17] and has been implemented in quantitative analysis.[17,22,33,35] However, in the cases considered so far the deviations from monoexponential behavior are rather small. Consequently, the amplitudes and time scales of motions extracted from relaxation rates are almost identical regardless of whether orientational dependence is included in the analysis. At the same time, inclusion of dependence of the relaxation rates on the orientation is not computationally costly and may become necessary to avoid errors in some cases, for example, when dealing with very slow anisotropic motions.

The emerging dynamic picture for globular proteins such as Crh,[17] SH3,[32] ubiquitin,[19] GB1,[22] and SOD[33] is similar to the picture painted by measurements in solution. Notably, larger amplitude motions are detected primarily in the loops and smaller amplitude motions in the β-sheets and helices. However, all of the SSNMR studies report detection of omnipresent small amplitude nanosecond motions that are not always detected in analogous studies in solution. There are still challenges associated with quantifying amplitudes of motions occurring on different time scales. For example, R_1 and $R_{1\rho}$ alone are not sufficient to constrain the amplitudes of fast picosecond motions but seem to be sufficient to get reasonable estimates of amplitudes for the nanosecond motions.[19,22,32,36] Constraining the overall amplitudes of motions with measured dipolar couplings (such measurements reflect the overall amplitude of motions from picoseconds up to the inverse of the coupling usually microseconds to milliseconds) improves the estimate of the amplitudes of fast picosecond motions (though sometimes the fast motion amplitudes determined in this way are larger than the analogous amplitudes determined in solution[36]). Molecular simulations also aid quantitative interpretation of the experimental dynamics data. In particular, molecular dynamics (MD) simulations are becoming increasingly important in this context with the first two studies that use MD to help quantify protein dynamics in crystals being a 50 ns MD of SH3[37] and a 200 ns MD of GB1.[36]

Beyond ^{15}N Relaxation and Toward Anisotropy of Motions

While ^{15}N relaxation is simple to analyze, it provides an incomplete view of protein dynamics. Only a few residues contain side-chain nitrogens, so even though side-chain ^{15}N relaxation provides valuable information about dynamics and the stability of peptides and proteins,[28] the obtained information is rather sparse. Moreover, since local motions in solids do not have to be disentangled from the overall motion, some of their aspects such as their directionality could be potentially easier to characterize in solids than in solution. However, NH bonds sample a limited set of directions and thus provide a limited scope for probing anisotropy (or directionality) of motions. ^{13}C relaxation naturally complements ^{15}N relaxation because it simultaneously allows extensive characterization of side-chain dynamics and often has a different spatial dependence on the directions of motions. Toward these aims, Lewandowski et al. introduced an approach for measuring ^{13}C spin−lattice relaxation in uniformly labeled proteins that relies on the fact that PDSD is significantly reduced by fast MAS.[18] Recently, we have extended $R_{1\rho}$ measurements to ^{13}C and used a combination of ^{13}C and ^{15}N relaxation for quantitative analysis of dynamics in the protein GB1 (to be published). Below we compare the ^{15}N and ^{13}C relaxation patterns recorded on GB1 in order to illustrate their complementary nature and to highlight the features suggesting directionality of motions. Figure 3 shows ^{15}N and ^{13}C relaxation rates measured on GB1 and projected onto its structure. To aid the reader in judging the spatial relationships between the different interactions whose fluctuations contribute to relaxation, we plotted in the figure NH (Figure 3a,d), CO (Figure 3b,e), and $C_\alpha H_\alpha$ (Figure 3c) bonds. In general, the same time scale and amplitude of rotations/fluctuations against axes positioned differently in space may result in different contributions to the relaxation rates. Figure 4 illustrates the simulated effect of different anisotropic motions of a peptide plane (assumed rigid) on ^{15}N and ^{13}C′ relaxation.

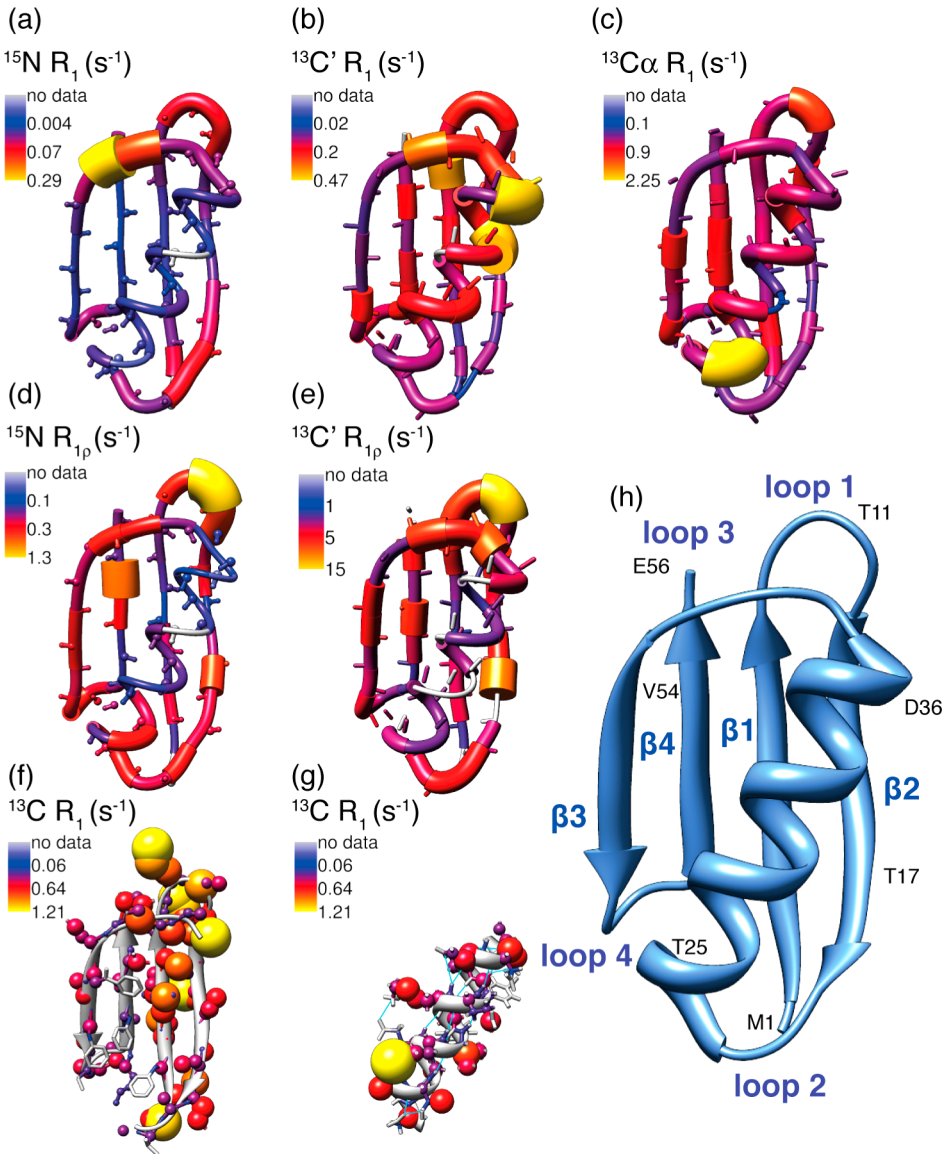

FIGURE 3. ^{15}N and ^{13}C relaxation rates measured in [U-^{13}C, ^{15}N]GB1.[18,22] R_1 and $R_{1\rho}$ rates are sensitive, respectively, to picosecond−nanosecond and picosecond−millisecond motions. The magnitude of the rates is indicated both by the radius of the "worm" (a−e) or sphere (f,g) (large radius, large rate) and color. All data were acquired at $\nu_r = 60$ kHz and ^{1}H Larmor frequencies of 1000 MHz (a, d), 800 MHz (b, c, f, g), and 850 MHz (e).

We observe that fluctuations against the axis parallel and perpendicular to the symmetry axis of the modulated interaction result in, respectively, a minimum and maximum contribution to the relaxation rate. For example, rotations of a peptide plane around the NH bond axis are not very effective in inducing ^{15}N dipolar and CSA relaxation but lead to effective ^{13}C′ relaxation because they modulate the σ_{xx} component of ^{13}C′ CSA.

All of the ^{15}N and ^{13}C rates in Figure 3 indicate increased mobility in loops 1 and 3. Since a peptide bond is to a good approximation planar, often the rate patterns are similar for the ^{15}N and ^{13}C′ located in the same peptide plane. For example, G41N and D40C′ that belong to the same peptide plane indicate the most mobile spot in the loop 3. In contrast, the fluctuations of ^{13}C$_\alpha$ are not restricted by the peptide plane geometry and thus can lead to a quite distinct rate pattern (but could be used to validate if the dominant motion is of a more global nature, see below). Small and relatively uniform ^{15}N R_1's throughout the helix suggest that it is rigid on the picosecond−nanosecond time scale. At the same time, both ^{13}C′ and ^{13}C$_\alpha$ R_1's indicate substantial picosecond−nanosecond mobility, sometimes larger than in the intrinsically more flexible loops. This discrepancy could be reconciled by considering rotations about an axis parallel to the long axis of the helix: NH bonds in a helix are roughly aligned with its long axis, but C$_\alpha$H$_\alpha$ bonds and σ_{xx} component of the ^{13}C′ CSA are

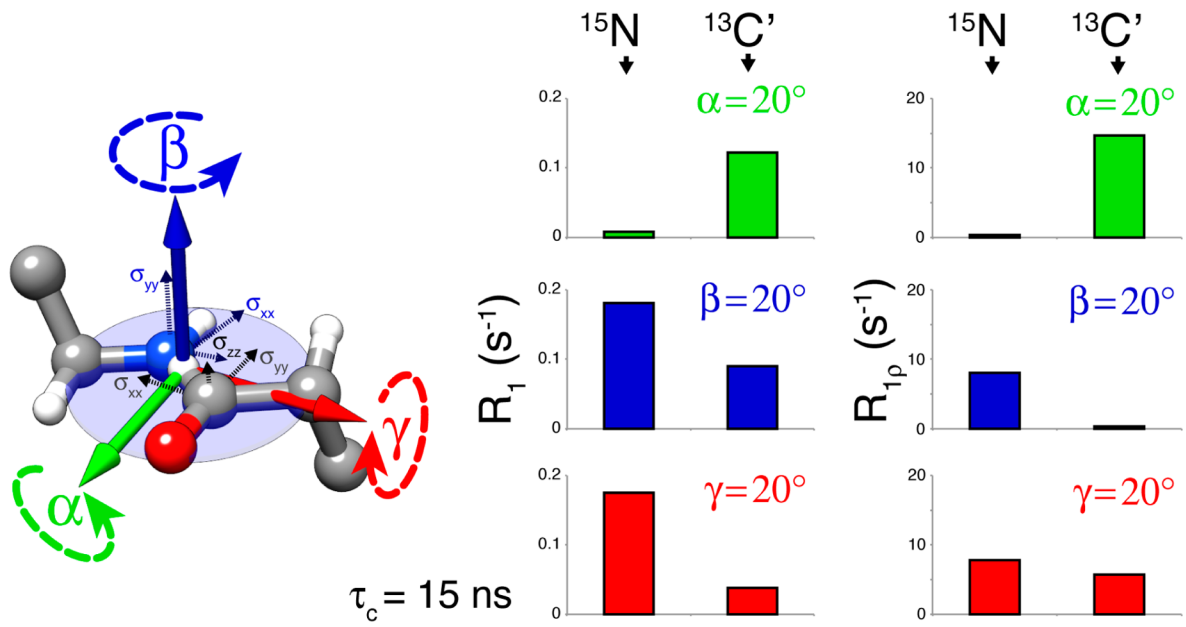

FIGURE 4. Effect of peptide plane anisotropic motion on ^{15}N and ^{13}C′ relaxation rates simulated at 850 MHz ^{1}H Larmor frequency using the simple model-free approach[32] with $\tau_c = 15$ ns and 3D GAF order parameter[38] resulting from 20° rotations/fluctuations against α, β, and γ axes. The dipolar vectors are collinear with lines connecting the atoms and the CSA components for ^{15}N and ^{13}C′ are indicated with dotted arrows.

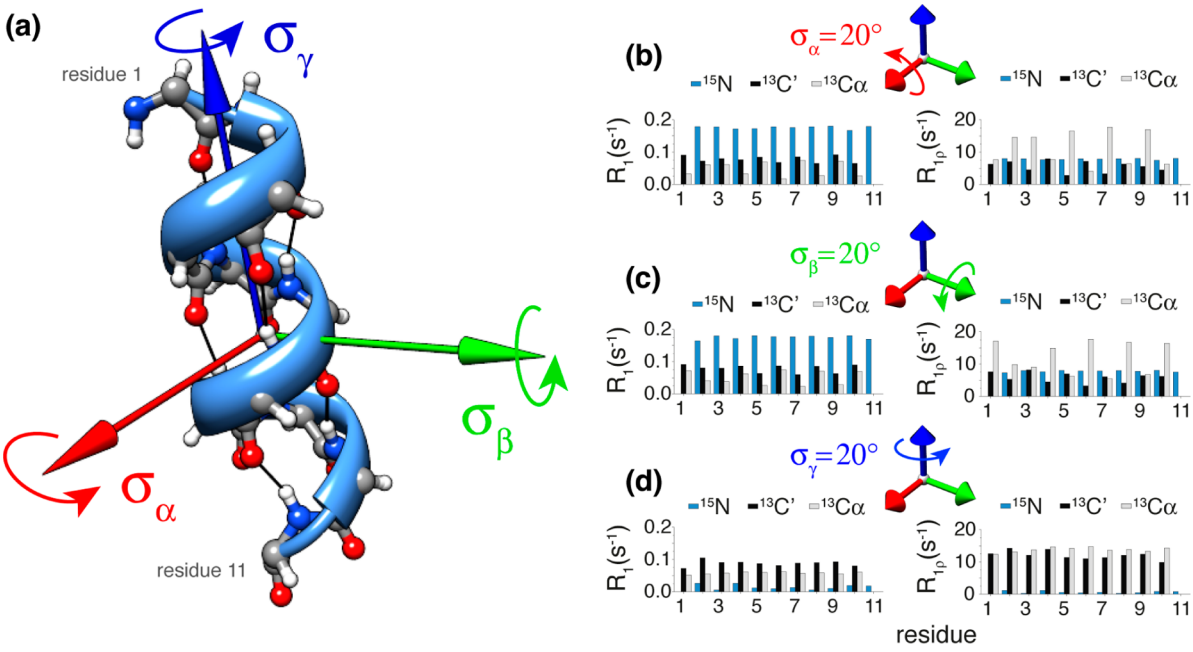

FIGURE 5. Effect of a collective anisotropic motion of a helix on the ^{15}N, ^{13}C′, and ^{13}C$_\alpha$ relaxation rates in different residues. The simulation details are similar to Figure 4.

almost perpendicular to it so the same motions would be effective in inducing ^{13}C$_\alpha$ and ^{13}C′ R_1 relaxation but less so for ^{15}N relaxation (see Figure 5d).

According to ^{15}N R_1 patterns the β_2 strand (and especially its C-terminus) is on average the most mobile of all the strands on the picosecond−nanosecond time scale. The higher-than-average picosecond−nanosecond mobility of β_2 seems to be also reflected in largest side-chain ^{13}C R_1's of all the strands. The opposite trend is observed from the perspective of ^{13}C′ and ^{13}C$_\alpha$ R_1. Such behavior could be again rationalized with anisotropic motions, an interesting notion since a correlated motion across the β-sheet was identified from the RDC measurement on the GB1 analogue, GB3.[39]

Recently, Lewandowski et al. showed that solid-state relaxation could be potentially interpreted in the context of small amplitude anisotropic collective motions of protein fragments.[35] When present, such slower nanosecond−millisecond motions would have a very pronounced effect on the solid-state relaxation rates (see Figure 5 where the effect of different anisotropic motions of a helix on relaxation rate patterns for its residues is demonstrated). In this way, experimental data could be sometimes analyzed in the context of collective modes of motion, greatly facilitating their functional interpretation.

Finally, it is interesting to compare the ^{15}N and ^{13}C′ $R_{1\rho}$ to what is known about slow motions and folding of GB1 from solution NMR and simulations. Residues with substantially elevated $R_{1\rho}$ rates in loop 1 and the N-terminal end of the helix were also identified as melting hot spots for GB1 unfolding.[40] The elevated $R_{1\rho}$ rates in the β_2 strand are consistent with the enhanced conformational sampling involved in the binding of GB3 with the antigen-binding domain of IgG.[39] Interestingly, ^{15}N and ^{13}C′ $R_{1\rho}$ are significantly elevated in peptide planes involving T53N and V54N, which are found near one of the nuclei in the penultimate step of GB1 folding.[41] In general, the structural elements involved in the folding pathway of GB1 seem to display a number of distinct features with respect to the detected slow motions. For example, based on ^{15}N relaxation the second β-hairpin ($\beta_3-\beta_4$) identified as the first folded element is characterized by overall slower motions than the first β-hairpin ($\beta_1-\beta_2$), which forms in one of the last steps.[22] It seems that elevated $R_{1\rho}$'s could help to outline "hinges" for significant structural rearrangement. This should be an extremely useful approach to identify primary motional modes for large conformational changes, even if the motions themselves are restricted either due to packing interactions or otherwise (such as in the case of β_4 strand in GB1).

Conclusion

In this Account, we discussed recent advances in solid-state ^{15}N and ^{13}C relaxation methodology for characterizing widespread site-specific protein dynamics. Solid-state relaxation provides simultaneously amplitudes and time scales of motions in the picosecond to millisecond range, covering a significant fraction of biologically important dynamic processes and including nanosecond−microsecond motions that are difficult to access otherwise. Solid-state relaxation also facilitates the characterization of directionality of motions, which is often important for understanding of their functional aspects. In addition to traditional SSNMR targets such as amyloid fibrils and membrane proteins, this methodology may facilitate understanding of dynamic processes in systems traditionally studied by other methods; for example, it may have enormous impact on characterization of site-specific dynamics in large molecular complexes. In the coming years, thanks to advances in solid-state relaxation methodology, easier sample preparation through sedimentation,[8] and increased sensitivity by ^{1}H detection under fast MAS,[11,33] we expect growing interest in SSNMR methodology for characterizing complexes.

I thank Jonathan Lamley for sharing ^{13}C′ $R_{1\rho}$ data on GB1 and careful reading of the manuscript. We acknowledge support of the EPSRC. We thank our collaborators Stephan Grzesiek, Hans Jürgen Sass, Martin Blackledge, and Lyndon Emsley for fruitful discussions. The U.K. 850 MHz solid-state NMR Facility used in this research was funded by EPSRC and BBSRC, as well as the University of Warwick, including via partial funding through Birmingham Science City Advanced Materials Projects 1 and 2 supported by Advantage West Midlands (AWM) and the European Regional Development Fund (ERDF).

BIOGRAPHICAL INFORMATION

Józef R. Lewandowski obtained his Ph.D. from Massachusetts Institute of Technology in 2008 for his work on development and applications of SSNMR for structural characterization of proteins in the group of Prof. R. G. Griffin. Subsequently, he worked with Prof. L. Emsley at ENS de Lyon as a Marie Curie Postdoctoral Fellow on development and applications of methodology for probing protein dynamics. In 2011, he became an Assistant Professor of Physical Chemistry at University of Warwick. His research interests include methodology development and applications of biomolecular NMR.

FOOTNOTES

The authors declare no competing financial interest.

REFERENCES

1 Henzler-Wildman, K.; Kern, D. Dynamic personalities of proteins. *Nature* **2007**, *450*, 964–972.
2 Frauenfelder, H.; Sligar, S. G.; Wolynes, P. G. The energy landscapes and motions of proteins. *Science* **1991**, *254*, 1598–1603.
3 Mittermaier, A.; Kay, L. E. New tools provide new insights in NMR studies of protein dynamics. *Science* **2006**, *312*, 224–228.
4 Lian, L. Y.; Middleton, D. A. Labelling approaches for protein structural studies by solution-state and solid-state NMR. *Prog. Nucl. Magn. Reson. Spectrosc.* **2001**, *39*, 171–190.
5 Martin, R. W.; Zilm, K. W. Preparation of protein nanocrystals and their characterization by solid state NMR. *J. Magn. Reson.* **2003**, *165*, 162–174.
6 Wasmer, C.; Lange, A.; Van Melckebeke, H.; Siemer, A. B.; Riek, R.; Meier, B. H. Amyloid fibrils of the HET-s(218-289) prion form a beta solenoid with a triangular hydrophobic core. *Science* **2008**, *319*, 1523–1526.
7 Loquet, A.; Sgourakis, N. G.; Gupta, R.; Giller, K.; Riedel, D.; Goosmann, C.; Griesinger, C.; Kolbe, M.; Baker, D.; Becker, S.; Lange, A. Atomic model of the type III secretion system needle. *Nature* **2012**, *486*, 276–279.
8 Bertini, I.; Luchinat, C.; Parigi, G.; Ravera, E.; Reif, B.; Turano, P. Solid-state NMR of proteins sedimented by ultracentrifugation. *Proc. Natl. Acad. Sci. U. S. A.* **2011**, *108*, 10396–10399.
9 Giraud, N.; Sein, J.; Pintacuda, G.; Bockmann, A.; Lesage, A.; Blackledge, M.; Emsley, L. Observation of heteronuclear overhauser effects confirms the N-15-H-1 dipolar relaxation mechanism in a crystalline protein. *J. Am. Chem. Soc.* **2006**, *128*, 12398–12399.

10 Heise, H.; Hoyer, W.; Becker, S.; Andronesi, O. C.; Riedel, D.; Baldus, M. Molecular-level secondary structure, polymorphism, and dynamics of full-length alpha-synuclein fibrils studied by solid-state NMR. *Proc. Natl. Acad. Sci. U. S. A.* **2005**, *102*, 15871–15876.

11 Lewandowski, J. R.; Dumez, J. N.; Akbey, U.; Lange, S.; Emsley, L.; Oschkinat, H. Enhanced resolution and coherence lifetimes in the solid-state NMR spectroscopy of perdeuterated proteins under ultrafast magic-angle spinning. *J. Phys. Chem. Lett.* **2011**, *2*, 2205–2211.

12 Takegoshi, K.; Nakamura, S.; Terao, T. C-13-H-1 dipolar-assisted rotational resonance in magic-angle spinning NMR. *Chem. Phys. Lett.* **2001**, *344*, 631–637.

13 Grommek, A.; Meier, B. H.; Ernst, M. Distance information from proton-driven spin diffusion under MAS. *Chem. Phys. Lett.* **2006**, *427*, 404–409.

14 Krushelnitsky, A.; Brauniger, T.; Reichert, D. N-15 spin diffusion rate in solid-state NMR of totally enriched proteins: The magic angle spinning frequency effect. *J. Magn. Reson.* **2006**, *182*, 339–342.

15 Giraud, N.; Blackledge, M.; Bockmann, A.; Emsley, L. The influence of nitrogen-15 proton-driven spin diffusion on the measurement of nitrogen-15 longitudinal relaxation times. *J. Magn. Reson.* **2007**, *184*, 51–61.

16 Chevelkov, V.; Diehl, A.; Reif, B. Measurement of (15)N-T(1) relaxation rates in a perdeuterated protein by magic angle spinning solid-state nuclear magnetic resonance spectroscopy. *J. Chem. Phys.* **2008**, *128*, No. 052316.

17 Giraud, N.; Blackledge, M.; Goldman, M.; Bockmann, A.; Lesage, A.; Penin, F.; Emsley, L. Quantitative analysis of backbone dynamics in a crystalline protein from nitrogen-15 spin-lattice relaxation. *J. Am. Chem. Soc.* **2005**, *127*, 18190–18201.

18 Lewandowski, J. R.; Sein, J.; Sass, H. J.; Grzesiek, S.; Blackledge, M.; Emsley, L. Measurement of site-specific C-13 spin-lattice relaxation in a crystalline protein. *J. Am. Chem. Soc.* **2010**, *132*, 8252–8254.

19 Schanda, P.; Meier, B. H.; Ernst, M. Quantitative analysis of protein backbone dynamics in microcrystalline ubiquitin by solid-state NMR spectroscopy. *J. Am. Chem. Soc.* **2010**, *132*, 15957–15967.

20 Muhandiram, D. R.; Yamazaki, T.; Sykes, B. D.; Kay, L. E. Measurement of ^{2}H T_1 and $T_{1\rho}$ relaxation-times in uniformly ^{13}C-labeled and fractionally ^{2}H-labeled proteins in solution. *J. Am. Chem. Soc.* **1995**, *117*, 11536–11544.

21 Chevelkov, V.; van Rossum, B. J.; Castellani, F.; Rehbein, K.; Diehl, A.; Hohwy, M.; Steuernagel, S.; Engelke, F.; Oschkinat, H.; Reif, B. ^{1}H detection in MAS solid-state NMR spectroscopy of biomacromolecules employing pulsed field gradients for residual solvent suppression. *J. Am. Chem. Soc.* **2003**, *125*, 7788–7789.

22 Lewandowski, J. R.; Sass, H. J.; Grzesiek, S.; Blackledge, M.; Emsley, L. Site-specific measurement of slow motions in proteins. *J. Am. Chem. Soc.* **2011**, *133*, 16762–16765.

23 Chevelkov, V.; Diehl, A.; Reif, B. Quantitative measurement of differential N-15-H-alpha/beta T-2 relaxation rates in a perdeuterated protein by MAS solid-state NMR spectroscopy. *Magn. Reson. Chem.* **2007**, *45*, S156–S160.

24 Tollinger, M.; Sivertsen, A. C.; Meier, B. H.; Ernst, M.; Schanda, P. Site-resolved measurement of microsecond-to-millisecond conformational-exchange processes in proteins by solid-state NMR spectroscopy. *J. Am. Chem. Soc.* **2012**, *134*, 14800–14807.

25 Kurbanov, R.; Zinkevich, T.; Krushelnitsky, A. The nuclear magnetic resonance relaxation data analysis in solids: General R-1/R-1 rho equations and the model-free approach. *J. Chem. Phys.* **2011**, *135*, No. 184104.

26 Krushelnitsky, A.; Reichert, D. Solid-state NMR and protein dynamics. *Prog. Nucl. Magn. Reson. Spectrosc.* **2005**, *47*, 1–25.

27 Helmus, J. J.; Surewicz, K.; Surewicz, W. K.; Jaroniec, C. P. Conformational flexibility of Y145Stop human prion protein amyloid fibrils probed by solid-state nuclear magnetic resonance spectroscopy. *J. Am. Chem. Soc.* **2010**, *132*, 2393–2403.

28 Lewandowski, J. R.; van der Wel, P. C. A.; Rigney, M.; Grigorieff, N.; Griffin, R. G. Structural complexity of a composite amyloid fibril. *J. Am. Chem. Soc.* **2011**, *133*, 14686–14698.

29 Ader, C.; Pongs, O.; Becker, S.; Baldus, M. Protein dynamics detected in a membrane-embedded potassium channel using two-dimensional solid-state NMR spectroscopy. *Biochim. Biophys. Acta, Biomembr.* **2010**, *1798*, 286–290.

30 Lorieau, J. L.; McDermott, A. E. Conformational flexibility of a microcrystalline globular protein: Order parameters by solid-state NMR spectroscopy. *J. Am. Chem. Soc.* **2006**, *128*, 11505–11512.

31 Yang, J.; Tasayco, M. L.; Polenova, T. Dynamics of reassembled thioredoxin studied by magic angle spinning NMR: Snapshots from different time scales. *J. Am. Chem. Soc.* **2009**, *131*, 13690–13702.

32 Chevelkov, V.; Fink, U.; Reif, B. Quantitative analysis of backbone motion in proteins using MAS solid-state NMR spectroscopy. *J. Biomol. NMR* **2009**, *45*, 197–206.

33 Knight, M. J.; Pell, A. J.; Bertini, I.; Felli, I. C.; Gonnelli, L.; Pierattelli, R.; Herrmann, T.; Emsley, L.; Pintacuda, G. Structure and backbone dynamics of a microcrystalline metalloprotein by solid-state NMR. *Proc. Natl. Acad. Sci. U. S. A.* **2012**, *109*, 11095–11100.

34 Redfield, A. G. On the theory of relaxation processes. *IBM J. Res. Dev.* **1957**, *1*, 19–31.

35 Lewandowski, J. R.; Sein, J.; Blackledge, M.; Emsley, L. Anisotropic collective motion contributes to nuclear spin relaxation in crystalline proteins. *J. Am. Chem. Soc.* **2010**, *132*, 1246–1248.

36 Mollica, L.; Baias, M.; Lewandowski, J. R.; Wylie, B. J.; Sperling, L. J.; Rienstra, C. M.; Emsley, L.; Blackledge, M. Atomic resolution structural dynamics in crystalline proteins from molecular simulation and NMR. *J. Phys. Chem. Lett.* **2012**, *3*, 3657–3662.

37 Chevelkov, V.; Xue, Y.; Linser, R.; Skrynnikov, N. R.; Reif, B. Comparison of solid-state dipolar couplings and solution relaxation data provides insight into protein backbone dynamics. *J. Am. Chem. Soc.* **2010**, *132*, 5015–5017.

38 Lienin, S. F.; Bremi, T.; Brutscher, B.; Bruschweiler, R.; Ernst, R. R. Anisotropic intramolecular backbone dynamics of ubiquitin characterized by NMR relaxation and MD computer simulation. *J. Am. Chem. Soc.* **1998**, *120*, 9870–9879.

39 Bouvignies, G.; Bernado, P.; Meier, S.; Cho, K.; Grzesiek, S.; Bruschweiler, R.; Blackledge, M. Identification of slow correlated motions in proteins using residual dipolar and hydrogen-bond scalar couplings. *Proc. Natl. Acad. Sci. U. S. A.* **2005**, *102*, 13885–13890.

40 Ding, K. Y.; Louis, J. M.; Gronenborn, A. M. Insights into conformation and dynamics of protein GB1 during folding and unfolding by NMR. *J. Mol. Biol.* **2004**, *335*, 1299–1307.

41 Kmiecik, S.; Kolinski, A. Folding pathway of the B1 domain of protein G explored by multiscale modeling. *Biophys. J.* **2008**, *94*, 726–736.